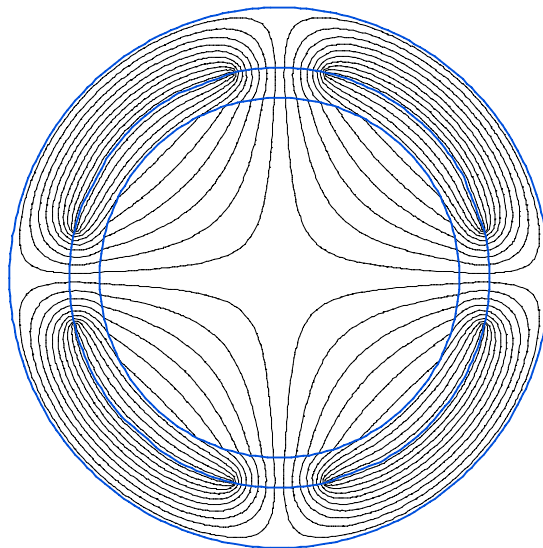# Capacitive measurement technique for void fraction measurements in two phase pipe flow

Bachelor project final report

Author: Mark Beker
               m.g.beker@student.tudelft.nl

Supervisors: dr.ir. Martin Rohde
               m.rohde@iri.tudelft.nl

               ir. August Winkelman   Delft
               a.m.j.winkelman@tnw.tudelft.nl   July 2005

Summary

This report describes the development of a capacitive void fraction senor. The sensor is designed to determine void fractions in two-phase pipe flow in the GENESIS (General Electric Natural circulation Experimental Scaled facility for the Investigation of Stability) project. Determining the void fraction in GENESIS is a crucial factor in understanding the stability of the system.

The void fraction can be determined by using a number of different techniques. Each of these techniques has its benefits and disadvantages. In this report some of these techniques will be discussed briefly and the development of the capacitive measurement technique will be outlined in more detail. A capacitive sensor has the benefit of being fast and non-invasive. A sensor has been developed with a number of requirements with regard to speed and accuracy in mind.

A static two-phase pipe flow model made of perspex was used to characterise the sensor. Using this model, different sensor concepts could be tested and the performance of the sensor could be investigated. The results of these tests have led to a sensor design with a resolution of 0.4% void. The accuracy of the sensor is 10-15% for unknown void distributions and 2-3% for known homogenous void distributions.

Table of contents

1 Introduction

1.1 Boiling water reactors

A boiling water reactor (BWR) is a nuclear reactor into which extensive research is being carried out. In particular, the reactors that incorporate natural circulation of the coolant form promising designs for future nuclear reactor plants. These reactors have shown an improvement in safety compared with traditional reactor types.

Both the BWR and the pressurised water reactor (PWR) are commonly used reactors at the moment. The biggest difference between the BWR and the PWR is the pressure at which the coolant water is contained. In a BWR this is about 70 atm compared with the 160 atm of a PWR. This decreased pressure means the water will boil at a lower temperature and is subsequently allowed to boil inside the reactor core. The generated water-vapour mix has a lower density and rises to the top of the reactor where the steam is extracted for electricity generation.

A new development in boiling water reactors is the incorporation of a natural circulation process. During this process the water that is separated from the steam, and the water from the steam that is condensed after electricity generation, are allowed to flow back to the bottom of the core on the basis of natural processes. This natural circulation process eliminates the need for pumps and ensures a simpler and safer design.

There are a number of aspects that play an important role in the safety and stability of the BWR. Especially the presence of steam makes a BWR a system that shows complex behaviour that may lead to instable behaviour. The most important processes that relate to the presence of steam are:
- the transport of heat from the fuel rods to the coolant (i.e. water),
- the flow characteristics in the core and the riser,
- the transport of neutrons (neutrons need to be decelerated by liquid water to induce fission of nuclear fuel)

The characteristics of the steam during this process are integral to monitoring the state and stability of the reactor. That is why it is important to be able to make accurate quantitative measurements of the amount of steam and water at certain points during the process. To do this the void fraction will be determined which is defined as the volumetric flow of gas divided by the total volumetric flow.

1.2 GENESIS

GENESIS stands for "General Electric Natural circulation Experimental Scaled facility for the Investigation of Stability". It is designed to investigate the behaviour of a natural circulation reactor (The so-called ESBWR). This behaviour is very complex to model numerically. However, by building a scaled experimental facility it is possible to investigate a number of aspects before a full

scaled facility is built and to compare these to the numerical results. GENESIS is scaled down in a number of ways, not only in size but also the temperature and pressure at which the cooling fluid exists. For this reason it is not possible to use water as the cooling fluid. A fluid is needed that behaves in the same way as water would in a real reactor but then at the temperature and pressure of GENESIS. That means a fluid that boils and condenses within the temperature and pressure bounds of GENESIS. GENESIS is therefore filled with Freon-R134a. Freon-R134a is a non-conducting fluid that boils at about 40 degrees Celsius at 6.5 bar. An important part of the investigation into the stability of the facility is determining the void fraction at certain points in the steam cycle. This is important in determining the steam production over time. This will be done at two points, one just after the core and one just before the steam separation vessel.

Figure 1.1 An illustration of the GENESIS facility where the top and bottom arrows indicate the steam separation vessel and reactor core respectively

1.3 Void fraction measurement techniques

In this paragraph some existing void fraction measurement techniques will briefly be discussed. Each of these techniques has its advantage and disadvantages for application in the GENESIS project.

Gamma ray absorption

The absorption of gamma rays by a material is dependant on the density of the material. The void fraction is directly proportional to the density of the two phase mixture. During a gamma ray absorption measurement, a small bundle of collimated gamma rays created by a source, are directed through the void to a detector on the other side. The intensity of the ray is determined on both sides of the void and the relationship between the two measurements gives a result for the void fraction using the following equation:

$$I = I_0 e^{-\mu d} \tag{1.1}$$

5

Where, I_0 is the intensity before and I the intensity after passage through the void. μ is the absorption coefficient of the liquid and d the distance travelled through the liquid. Using d the void fraction can be found.

The major disadvantage of this technique is that it only gives an averaged void fraction across a small cross-section of the void and not a volumetric one. The speed of the measurement is also bounded by the nature of the radiation source. For an accurate measurement one needs a strong source or a long measurement time. If the source is not strong enough the detected signal will be weak, giving less accurate results. This can be helped by detecting the signal over a longer period, bringing with it the disadvantage that each measurement will take more time and become insensitive to smaller fluctuations of the void in the time. Because the source and detectors are situated on the outside of the pipe, much of the useful radiation may be absorbed depending on the thickness and properties of the container material.

X-ray absorption
The X-ray absorption technique works in a similar way to that of gamma ray absorption. The higher intensity of the x-rays solves the problems of time resolution and accuracy. This does however bring with it the extra problem of shielding and health risks. As well as this the relationship between the void and the absorption of x-rays is not a simple monochromatic relationship which ensures complicated calculations of the void fraction.

Impedance
The impedance can be measured by inserting two probes into the void flow. The impedance measured in a two-phase mixture changes if there is liquid or vapour around the sensor. The void fraction is determined by measuring over a certain period to get a time averaged void fraction. One therefore needs to measure over a long period in order to get a reliable average. This is disadvantageous when frequent measurements are required. This technique is cheap and is excellent for local void fraction results but cannot be used for volume averaged void distribution measurements. Inserting probes into the void flow is disruptive for the flow of the mixture. The most obvious disadvantage is of course that it cannot be used for measurements in non-conducting fluids.

Optical void probes
Optical void measurement techniques make use of Snell's law, which suggests that the refraction and reflection of light is dependent on the refraction index of the materials between which the refraction takes place. The refraction index is also dependent on the void fraction, so that by measuring the reflection and refraction of light at the end of a probe, the void fraction can be determined. This technique has the benefit that it can be used for conducting and non-conducting fluids. However, it is intrusive and only suitable for local void fraction measurements.

2 Capacitive measurement technique

2.1 Definition of capacitance

Two conducting bodies are placed in the vicinity of each other. One conductor is charged with a charge +Q and the other with a charge –Q. Each conductor then has a resulting electric potential V. We can therefore speak of a potential difference between them:

$$V = V_+ - V_- = -\int_{(-)}^{(+)} \overline{E} \bullet d\overline{l} \qquad (2.1)$$

V and E are both proportional to the charges on the conductors according to:

$$V(r) = \frac{1}{4\pi\varepsilon_0} \int \frac{\rho}{\xi} d\tau \qquad (2.2)$$

$$E(r) = \frac{1}{4\pi\varepsilon_0} \int \left(\frac{\hat{\xi}}{\xi^2} \right) \rho d\tau \qquad (2.3)$$

where ρ is the charge per unit volume.
The constant of proportionality as a result of the relation between *E*, *V* and Q is known as the capacitance of the arrangement:

$$C = \frac{Q}{V} \qquad (2.4)$$

In a vacuum capacitance is a purely geometrical quantity, determined by the sizes, shapes and separation of the conductors. It is useful to describe the situation in the form of a differential equation; this can be done using Poisson's equation.

$$\nabla^2 V = -\frac{1}{\varepsilon_0} \rho \qquad (2.5)$$

Poisson's equation describes a boundary value problem; therefore it's solution depends on the boundary conditions within and on the boundary of a closed region where the equation is to be solved.
For the special case of two parallel plates of area *A*, separated by a distance *d* of vacuum, one plate carries a surface charge density +σ, and the other – σ. We assume that the electric field *E* between the plates is uniform (and zero elsewhere), we may write $E = \dfrac{\sigma}{\varepsilon_0}$. The potential difference between the plates is given by

$$V = Ed = \frac{Q}{\varepsilon_0 A} d \qquad (2.6)$$

from which the capacitance can be found to be:

$$C = \frac{\varepsilon_0 A}{d} \qquad (2.7)$$

2.2 Effect of a dielectric

Up until now we have discussed capacitance for conductors surrounded by vacuum. When the vacuum is replaced by a dielectric material the capacitance will increase by a factor ε_r, which is called the dielectric constant of the material. To understand this effect it is necessary to introduce the concept of polarisation and bound charges. Polarisation occurs within the material and is thus dependant on the material properties. This polarisation is a result of microscopic displacements of charge at an atomic or molecular level. Poission's equation has no parameters that are material dependant so the result will not change between the vacuum and non-vacuum solutions. To account for the change in capacitance it is necessary to make a distinction between free and bound charges. The bound charge is the charge as a result of the polarisation of the dielectric at the boundary between the two media of different dielectric constants. The free charge is the charge on the surface of the conductor. This charge is free to move on the conductor and is the charge we measure when measuring the capacitance. Both types of charges are present at the boundary between conductor and dielectric.

For a linear isotropic medium the polarisation is given by

$$\vec{P} = \varepsilon_0 (\varepsilon_r - 1)\vec{E} \qquad (2.8)$$

where $\vec{P}$ is the polarisation and ε_o the permittivity of free space. The bound charge caused by the polarization is given by

$$\sigma_b = \vec{P} \cdot \hat{n} \qquad (2.9)$$

Combining equations (2.8) and (2.9) results in the following expression for the bound charge

$$\sigma_b = \varepsilon_0 \varepsilon_r \vec{E} \cdot \hat{n} - \varepsilon_0 \vec{E} \cdot \hat{n} \qquad (2.10)$$

Gauss's law provides us with a relationship between the total charge and the electric field; $\sigma_t = -\varepsilon_0 \vec{E} \cdot \hat{n}$.(Griffiths [2]) Bearing this in mind, and the fact that the total charge is the sum of the bound and free charges, it can be concluded that for the free charge:

$$\sigma_f = -\varepsilon_0 \varepsilon_r \vec{E} \cdot \hat{n} \qquad\qquad (2.11)$$

This is indeed in accordance with what was mentioned earlier, that the capacitance is increased by a factor ε_r.

2.3 Effect of flow patterns

It has been shown that changing the dielectric constant of the medium between two plates of a capacitor will change the capacitance that is measured. The objective of the sensor however is to determine the void faction of a certain volume of two phase flow.

In general, the dielectric constant of vapour is much smaller than that of liquid water or liquid Freon-R134a. The higher the void fraction, the more vapour is present in the mixture, resulting in a lower effective dielectric constant and a lower capacitance. Unfortunately it is not so simple. The volumetric void fraction only indicates an average of the volume of space while the capacity depends on the distribution of the void within the volume as well. This means without any knowledge of the void distribution it is not possible to determine the capacity and vice versa with a capacitance measurement it is not possible to determine the void fraction. The void pattern can be roughly characterised by the average bubble size and the distribution of the bubbles. Examples of common flow patterns are; bubbly flow, annular flow and slug flow. A solution to this problem is to assume a certain flow pattern and calibrate the sensor accordingly. The disadvantage of this method is that prior knowledge of the flow is required, which in practice is often not possible and flows that do not correspond to the chosen flow pattern will give inconsistent results.

Taking a closer look at the bubbly flow distribution it is possible to distinguish different void distributions. The way in which the bubbles are 'aligned' with the electric field will also influence the capacitance. The bubbles can be homogenously distributed throughout the volume of space or they could be aligned perpendicular or parallel to the electric field, Figure 2.1 illustrates this idea:
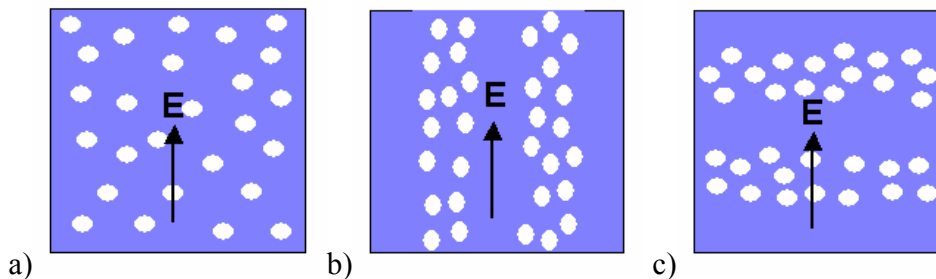

a)   b)   c)

Figure 2.1 Void distribution of bubbles a) Homogenous b) Parallel c) Perpendicular to electric field

In the case of parallel distribution the bubbles are aligned before and after each other resulting in a weaker relative electric field than in the homogenous case. In the case of a perpendicular distribution, the opposite is true. The perpendicular and parallel examples of the void distribution are two extremes of what would be expected, as shown by Kok[1]. When simulated in the outmost extreme case, where each alignment of bubbles is represented by a ridged area with a different dielectric constant to its surrounding medium, it is easy to calculate the effective dielectric constant of these flows. In the parallel case the total capacitance can be considered to consist of several capacitors connected in parallel while in the perpendicular case they are connected in series. The effective dielectric constant for series connection can be calculated to be,

$$\varepsilon_{eff} = \alpha + (1-\alpha)\varepsilon_r \qquad (2.12)$$

While for a parallel distribution it is,

$$\varepsilon_{eff} = \frac{\varepsilon_r}{\varepsilon_r \alpha + (1-\alpha)} \qquad (2.13)$$

These two extreme cases are plotted in Figure 2.2. Any bubbly flow will fall between these two values. These flow types therefore give us an indication of the maximum error that can be made in the measurement of the void fraction if the flow type and distribution is unknown.
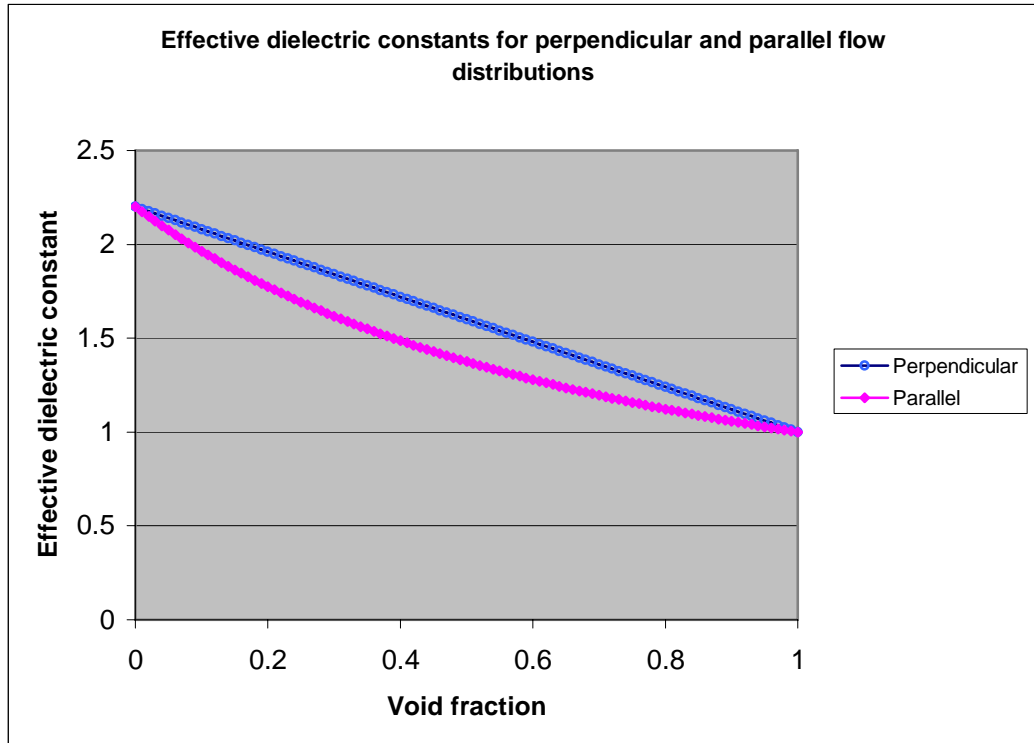
Figure 2.2 Effective dielectric constants for perpendicular and parallel flow distributions, ε_r is taken to be 2.2

By assuming a series distribution (equation(2.12)) the relationship between the capacitance and the void fraction can be considered linear. This is also due to the fact that the effective dielectric constant and capacitance are proportional to each other (see Equation 2.7). Bearing this is mind the following equation can be formulated for the void fraction, α

$$\alpha = \frac{C_l - C_m}{C_l - C_v} \qquad (2.14)$$

Where C_l is the capacitance of the sensor filled with only liquid, C_v the capacitance of the sensor filled with only vapour and C_m the capacitance of the mixture of the two phases. To better understand the origin of equation (2.14) one could rearrange it in terms of the measured capacitance,

$$C_m = C_l - (C_l - C_v)\alpha \qquad (2.15)$$

This equation shows that when the void fraction is 0, the measured capacitance will be that of C_l and when the void fraction is 1 it will be that of C_v. For all other values of α, C_m will fall in linear line between these two points. This equation is most accurate for series void distributions in a homogenous electric field and can only be used as an approximation of the actual void. The extent of the error involved in making this approximation will be investigated later in this report.

3 Sensor design strategy

3.1 Introduction

The theoretical basis for the capacitive sensor has been discussed thoroughly. It is now time to turn to the actual design of the sensor. There are three main aspects of the sensor that have been investigated in depth. The first of these to be discussed is the physical geometry of the sensor. The number of conducting plates, and the way in which they are charged and orientated around the pipe, play a crucial role in the performance of the measurements. The geometry also determines to a large extent the electric field distribution in and around the sensor, which is the second topic of discussion in this chapter. The third main aspect that involved a lot of design and development was the electronics that were used to control the sensor and read out the measurements. There are some requirements to which the sensor must conform in order to be effective in the desired situation. These factors are important in determining the eventual design of the sensor and will also be mentioned throughout this chapter.

3.2 Sensor Geometry

The sensor electrodes were designed in such a way that void fraction changes throughout the whole cross-section of the pipe would have a similar effect regardless of the location. For this purpose the electric field distribution was investigated for different sensor geometries. There will be more detail on this subject in the following paragraph. The requirements for the spatial resolution also demanded some thought. The electrodes had to create a capacitance that could be reasonably well detected. Research has been carried out into different electrode shapes and configurations, Abouelwafa, Kendall [3]. Here it was concluded that configurations with 2 large electrodes placed opposite each other or 4 smaller electrodes equally spaced around the pipe gave the best results. For the 4 electrode sensor there are 2 possible charge configurations, these being; opposite pairs, where two electrodes opposite each other have the same potential, whilst the other two have an equal but opposite potential. And adjacent pairs, where the electrodes are grouped two next to each other. These configurations of 2 and 4 electrodes will be investigated in detail throughout the rest of the paper.

3.3 Electric field distribution

The importance of the distribution of the electric field has already been mentioned earlier. For the measurements to be as reliable as possible for each void distribution, it is important that the electric field distribution is as homogenous as possible. To get an idea of how the electric field behaves in the sensor computer simulations were made. Initially a simple matlab programme was made that assumed that the electrodes could be described as a large number of point charges. According to the following equality the electric field could be determined in a simplified 3-dimensional model of the sensor:

$$|E| = \frac{1}{4\pi\varepsilon_0} \sum_i \frac{q_i}{r_i^2} \qquad (3.1)$$

A visualisation of this simulation for a 2-electrode configuration where the electrodes have the same but opposite potential can be seen in Figure 3.1.
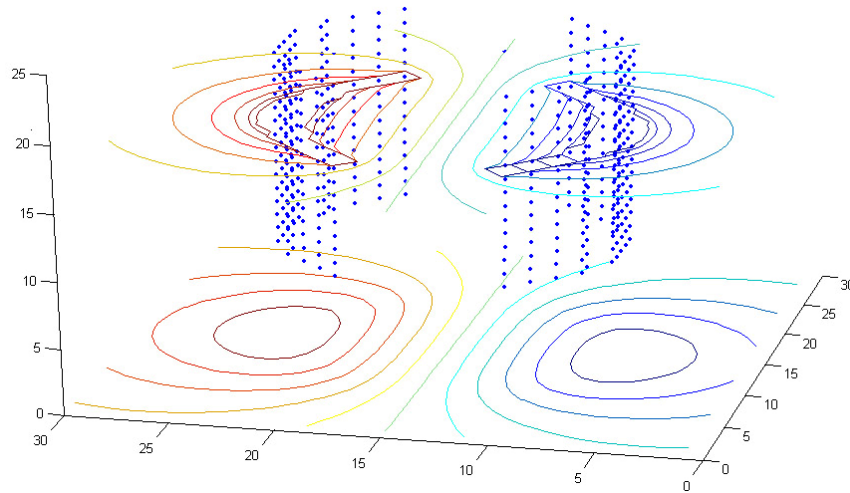
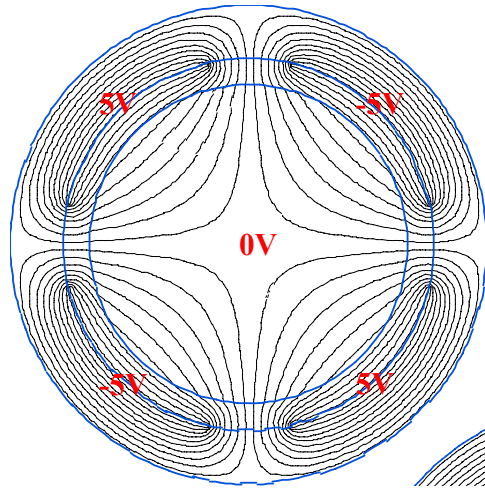**Figure 3.1 Matlab simulation of electric field distribution for 2 electrode sensor**

As it appears in Figure 3.1 the electric field radiates a long way out from the sensor. This means that there could be disturbances in the electric field and capacitance measurements from external factors such as other conductors or movement in the laboratory. The most logical solution to this problem is the use of a guard electrode that encompasses the entire sensor. The guard electrode is set to ground (zero voltage). The effect of a guard electrode on the electric field distribution also required modelling. However the inclusion of the guard electrode increased the complexity of the problem so that it could no longer be solved by the simple assumption of point charges. A finite element method was adopted in the form of a programme called Quickfield. Quickfield was only available in the limited student version that could only solve problems using up to 210 nodes. With this programme different geometries could be created using lines, circles and blocks. A number of properties could be attributed to each area in the resulting geometry, including electric permittivity, electric potential and charge. The results of the simulations for a two electrode system with a guard electrode set to zero potential are shown in the following illustrations;

13

a)

b)

c)
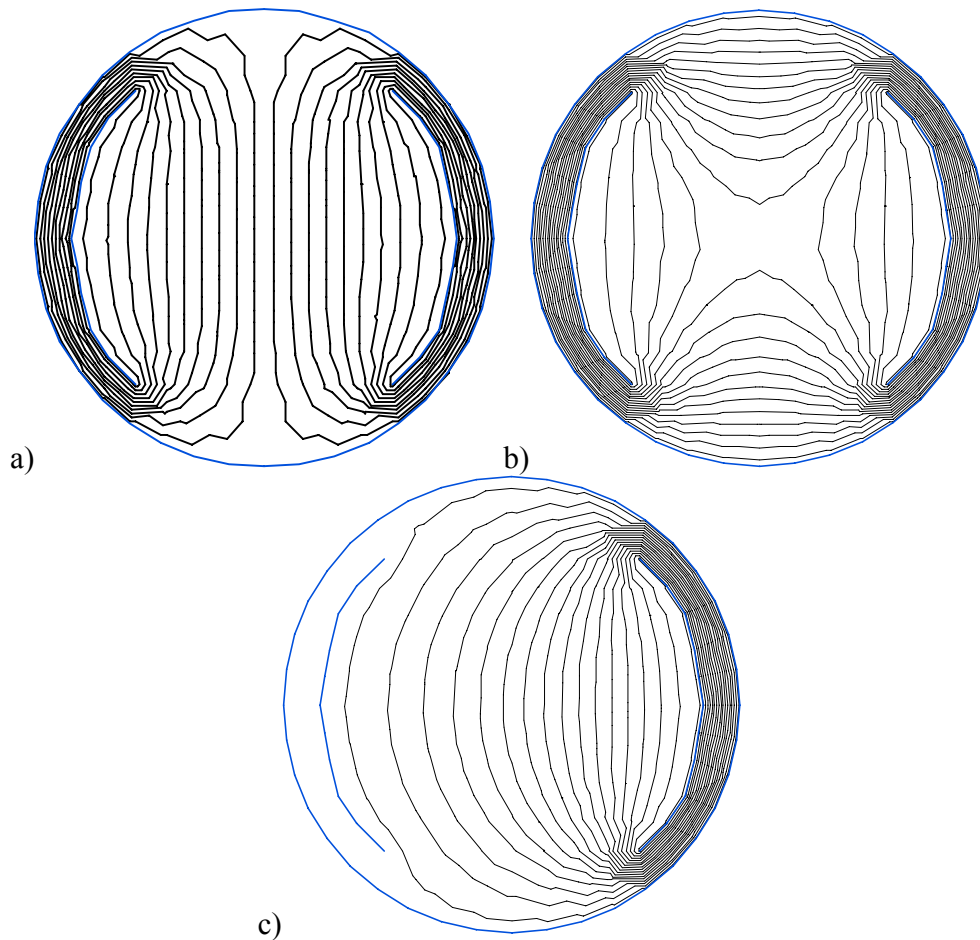
Figure 3.2 Quickfield model of 2 electrode sensor with guard at ground potential for a) equal and opposite charges b) both electrodes set to a positive charge and c) left electrode set to 0. The lines shown are equi-potential lines that run perpendicular to the direction of the electric field. The closer the lines are together the stronger the electric field.

It is clear that the guard electrode has the desired effect. In the definition for capacitance an example was used where each conductor had the same but opposite charge. This doesn't necessarily need to be the case. In Figure 3.2 b) the electric field distribution is shown for the situation where both electrodes have the same potential and in Figure 3.2 c) for the situation where one electrode is set to zero potential. These simulations show that the homogeneity of the electric field varies greatly between the different configurations and is optimal when the electrodes are set to equal but opposite potentials, as in Figure 3.2 a).

It was also possible to send a problem description away to be solved by the professional version of Quickfield providing better resolution for more complex geometries. The situation for 4 electrodes with opposite pairs was simulated in this way as shown in Figure 3.3.

Figure 3.3 Quickfield simulation of 4 electrode opposite pairs sensor. The lines shown are equi-potential lines that run perpendicular to the direction of the electric field. The closer the lines are together the stronger the electric field.

It included the glass wall of the pipe with a different dielectric constant than that of vapour or void. The effective dielectric constant was taken as 9, that of Freon-R134a, whilst the glass and vapour had a dielectric constant of 4 and 1 respectively. Figure 3.3 shows that there is no electric field in the centre of the pipe. The sensor would therefore feel no effect to changes in the void at the centre of the pipe.

3.4 Electronics

As we discovered in the previous chapter, bipolarity of the two electrodes is an important factor in insuring a homogenous electric field. It is therefore also essential that the electronics be designed with this as a key requirement. Another requirement was that the measurements could be made quickly. In GENESIS the measuring frequency is 500Hz which means 1 measurement every 2 milliseconds. The sensor had to be sensitive enough to detect tiny fluctuation in capacitance as small as 0.1 pF. The resulting design that was thought to comply with all these requirements was based on an RC-oscillator circuit. Such an oscillator has the benefit of producing a capacitance dependant frequency that can be easily and accurately detected using a data-acquisition card connected to a computer. An RC-oscillator circuit also provides a very simple relationship between the frequency and capacitance, as shown in Baxter [4],

$$f = \frac{1}{2.2RC} \qquad (3.2)$$

A simplified illustration of the final electronics circuit is given below.
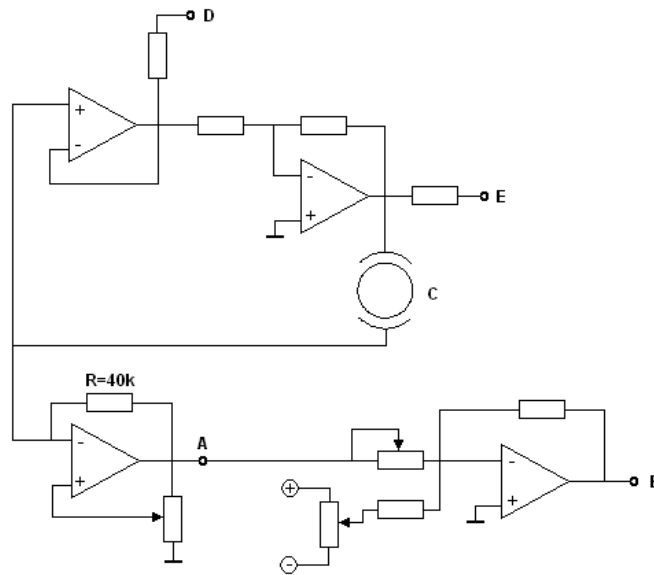
Figure 3.4 Illustration of final electronics circuit with probe points A, B, D and E used to check the signal throughout the circuit. Most resistor values are left out for simplification.

The probe locations D and E are purely used to check the voltage potential over the electrodes of the sensor. These should be dipolar as illustrated in Figure 3.5 below. The output at A is a block signal that switches between +½V and –½V, where V is the supply voltage of the operational amplifiers (op-amps). To be able to determine the frequency with a data-acquisition card the signal must oscillate between zero and a positive voltage, in this case approximately 3V. This is achieved using a non-inverted amplifier with a variable dc offset. The signals that are measured at points A and B are also shown in Figure 3.5 below.
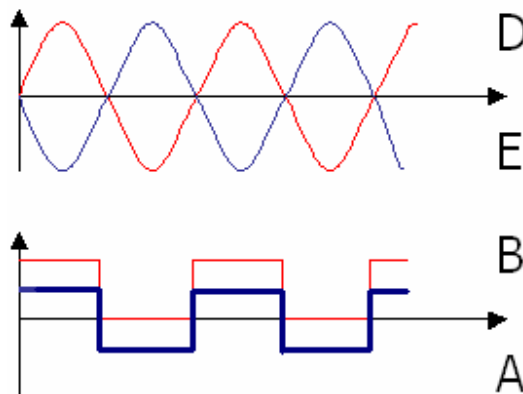
Figure 3.5 Schematic representation of signals throughout circuit, D and E represent the signals on the two electrodes from the oscillator, A the output signal of the oscillator and B the output after the non-inverted amplifier.

Frequency measurements are being made whilst it is the capacitance or the void fraction that we want to determine. Because of the inverse linear relationship

16

between the frequency and capacitance equation (3.2) and (2.14) can be combined to give:

$$\alpha = \frac{\dfrac{f_l}{f_m} - 1}{\dfrac{f_l}{f_v} - 1} \qquad (3.3)$$

Where f_l is the frequency of the sensor filled with only liquid, f_v the frequency of the sensor filled with only vapour and f_m the frequency of the mixture of the two phases.

4 Measurements

4.1 Apparatus

Using the information acquired during the modelling phase of the project we now have a good idea as to how the sensor should be designed. There are however still a number of aspects that need to be explored in more detail with experimental methods. For example experimental results could provide general information about how well the sensor worked with 2-electrodes compared to one with 4 electrodes. But more importantly using experimental methods it is possible to determine the effectiveness of the sensor by comparing experimental results with theoretical expectations.

To do this a void model or phantom void has been constructed out of Perspex and a glass pipe. The purpose of the phantom void is to create a static void distribution to simulate that of liquid and vapour in a two-phase pipe flow. Perspex has a dielectric constant of circa 3, whilst that of air is about 1. Therefore a piece of Perspex in a volume of air will act like a 'bubble' of liquid. To be able to simulate many different void distributions the volume inside the pipe (between the electrodes) needs to be able to be divided into sections of void (no Perspex) and liquid (Perspex). To do this there are two possible Perspex test sections. The first is a full Perspex cylinder that has been divided into 5 segments of equal volume (Figure 4.1a), each segment is therefore 20% of the total volume. The second is a collection of 37 small rods that run parallel to the pipe (Figure 4.1b). Each rod represents 1.3% void fraction. Perspex holders hold the rods in place at the ends of the glass pipe. When all the rods are inserted into their positions, the void fraction (the air between the rods) is about 50%. By removing rods the void can then be varied between 50 and 100%.

a)   b)
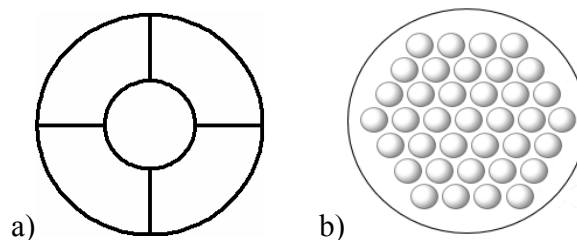
Figure 4.1 Perspex void distribution models a) 5 segments of equal volume b) 37 rods

The electronic circuit described in paragraph 3.4 has been incorporated into a metal box to reduce any external noise effects. The electrodes are secured to the outside of the glass pipe with non-conducting tape. The wires that connect to the electrodes are twisted around each other to reduce parasitic capacitances and movement between the two wires. The supply voltage is connected to a power supply generator with a +5V and -5V output supply. The guard electrode fits around the glass pipe and electrodes and can be secured there with plastic screws. Figure 4.2 is a photo of the experimental apparatus with the rod void model

inserted into the glass pipe. The guard has been removed but can be seen behind the sensor.
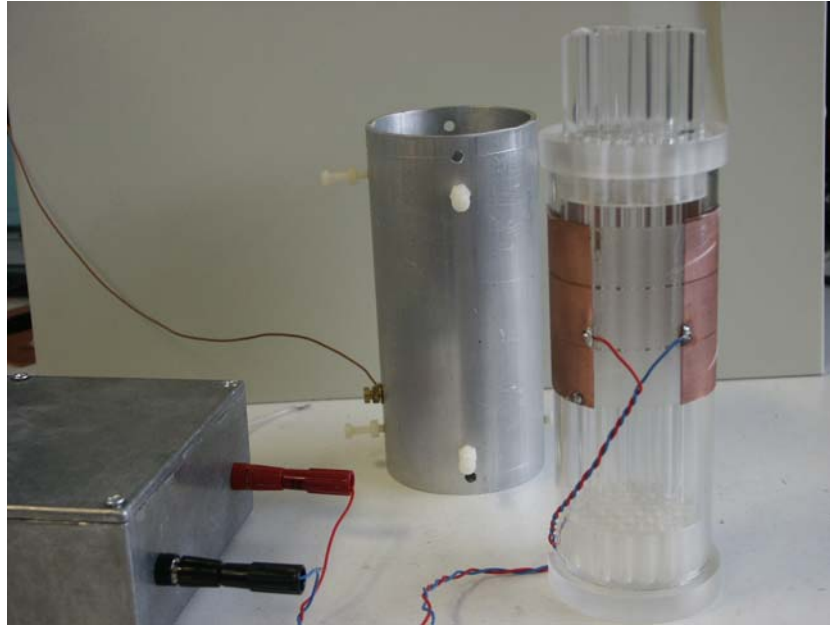

Figure 4.2 Photo of experimental apparatus with the rod-void model and the guard removed.

The output signal is transported via a coaxial cable to a 16 bit DQ-mx series data acquisition card in a computer. Using the programme LabView one can determine the frequency that is generated by the sensor.

4.2 Void fraction

To get an idea of how the sensor responds to changes in the void at different locations in the flow the rod-void model can be used. The relative change in capacitance due to the removal of a rod at that location can be calculated. To do this a measurement must be taken before and after a rod has been removed. By removing the rods one by one without replacing them, it is possible to determine how the capacitance changes with respect to the void fraction. As mentioned in 2.3 this should be a linear relationship. This change is also dependent on the order in which the rods are removed as each rod has an influence on the others. To try and create a 'series' and 'parallel' configuration the rods where removed as shown in Figure 4.3.
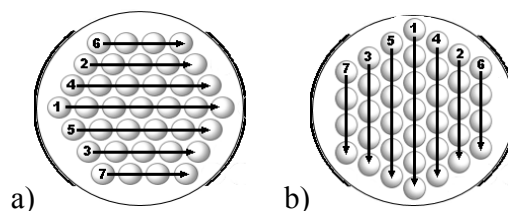
Figure 4.3 Order in which the rods are removed for a) parallel and b) series distributions

4.3 Homogeneity

The importance of the homogeneity of the sensor has been mentioned a number of times before. It will be interesting to see the effect of removing a rod at each location one by one. This can give us a better idea of the effect of a change in void at that particular location and a better insight into the homogeneity of the sensor. A similar approach is used as in the previous paragraph - only each rod is returned to its original position after a measurement has been made.

4.4 Effect of void distribution

The effect of the void distribution can best be simulated using the 5 segment void distribution. If, for example, two of the segments are placed in the pipe the effective void fraction will be 60%. There are 8 different combinations of the 2 segments in the 5 locations, thereby keeping the void fraction the same for each combination. Theoretically the void fraction stays the same for each combination. The void fraction can be measured and compared with the expected value to get an idea of the effect of the void distribution and the error involved as a result of different void distributions.

4.5 Bubbly void distribution

To determine the effect of the bubble size on the measurements we can once again use the rod-void model. By removing twelve rods a void fraction of about 84.4% is simulated. These vacant rod positions can be arranged into groups of 1, 3, 4, 6 and 12, thus creating five different configurations. Each configuration represents respectively 12, 4, 3, 2 and 1 bubble(s) of different sizes. These configurations are shown graphically in Figure 5.4. Once again the theoretical void fraction stays the same for each configuration so we can determine the measurement error as an effect of varying bubble size.

4.6 Measurement error

Another important aspect that needs to be investigated is the error involved in the measurement itself. If a measurement is made for a certain void fraction, the same measurement should be obtained again for that same void fraction. The possible fluctuations in the results of identical measurements could be a result of instabilities in the measuring apparatus. These could be caused for example, by uncertainties in the measuring equipment, resolution of measuring equipment and/or external factors such as electrical noise or parasitic capacitances. To determine a quantitative indication of the measurement error the detection limit will be determined. In general the detection limit of a sensor can be expressed in terms of the standard deviation, σ of repeated measurements. Often the detection limit is taken to be 2σ. It is also possible that measurements are temperature dependent which could also lead to fluctuations in measurements over a longer period of time.
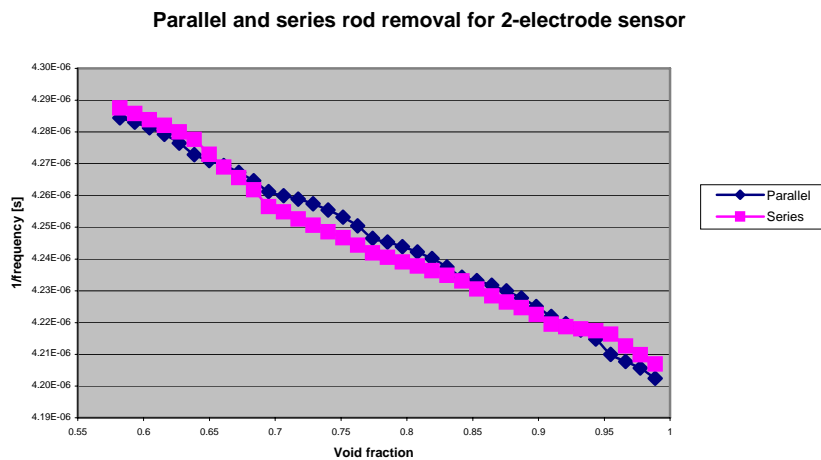
5 Results

5.1 Void fraction

The results for removing the rods one by one without replacing them are shown below.
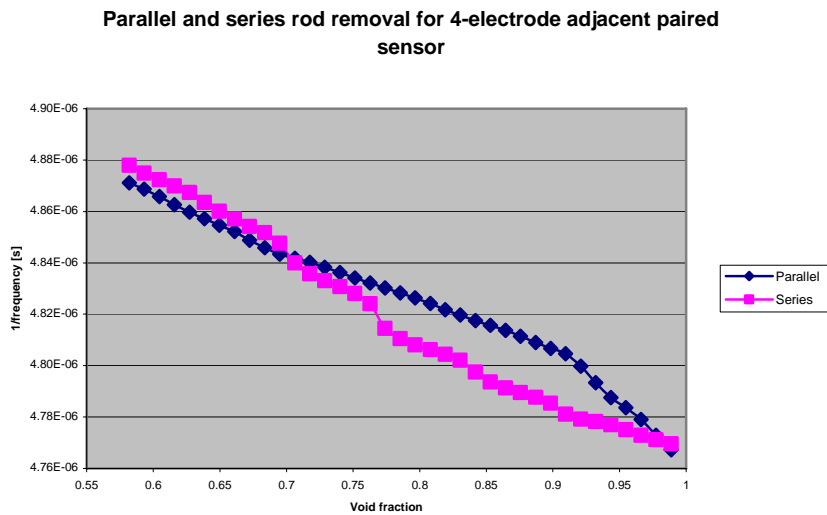
a)

b)

Figure 5.1 1/frequency verses void fraction for parallel and series removal for a a) 4-electrode adjacent paired sensor and b) a 2-electrode sensor

In Figure 5.1 the linear relationship between the capacitance and the void fraction can be clearly seen. Figure 5.1 a) shows that the parallel and series removal deviate from each other and from any linear approximation. This goes to show the order in which the rods are removed is of great importance and could influence the results. For any one measurement made the actual void could lie between the two extreme cases, parallel or series. The maximum distance between these two

curves is 9% void. This distance is much smaller for the 2-electrode sensor, approximately 3%.

5.2 Homogeneity

Now we would like to get an idea of the effect each rod has on the capacitance with respect to the other rods. In this way it is possible to illustrate the homogeneity of the sensor. In a homogeneous field each rod should have the same effect on the measurement. To do this the change in capacitance due to the removal of that rod is calculated and the results plotted in a surface plot where the height indicates the extent of the change. The values have also been normalised to the maximum value in each experiment. These plots are shown in Figure 5.2 for various measurements.
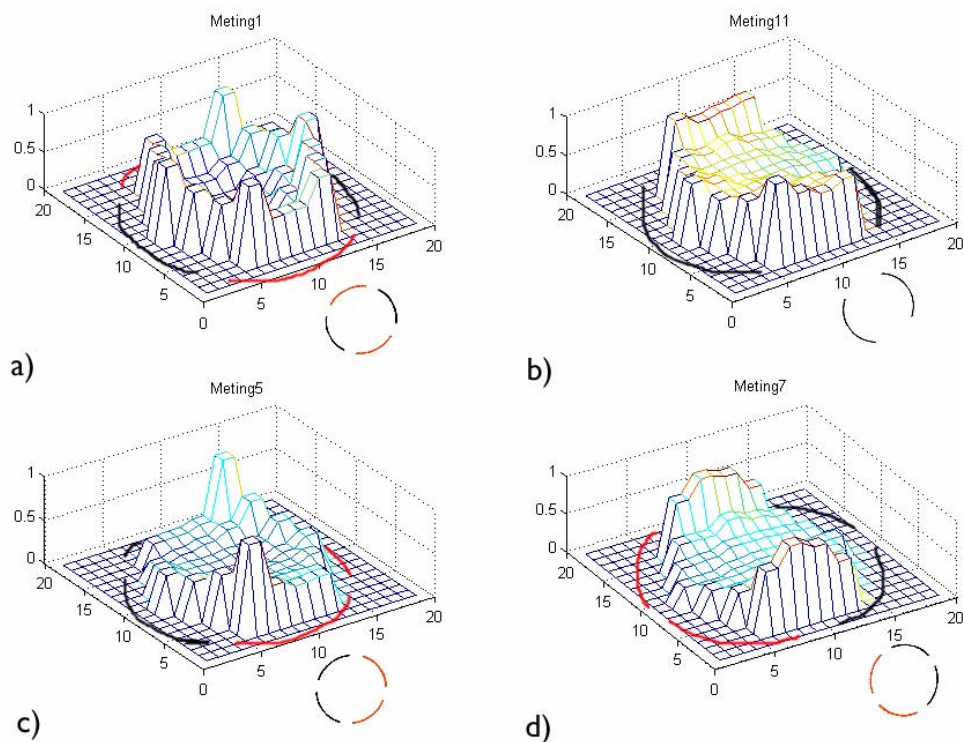
Figure 5.2 Relative changes in capacitance for each rod for a) opposite paired 4-electrode sensor b) 2-electrode sensor c) adjacent paired 4-electrode sensor d) adjacent paired 4-electrode sensor with different orientation. The orientation and charge of the electrodes are indicated by the insets and drawn around the plots.

As shown earlier, the electric field density in the middle of the pipe for an opposite paired 4-electrode sensor is zero. As expected Figure 5.2a reveals that the relative change at that position is also zero. This is improved for the adjacent paired 4-electrode sensor (Figure 5.2c and d) however they also show large peaks at the position near to where the two oppositely charged electrodes meet. This is logical as it is in these positions that the electric field is the strongest. For need of a quantitive analysis of the homogeneity the variance for each plot was calculated. This gives a quantitive figure for the homogeneity where the smaller the variance

the better the homogeneity. The variances for each experiment are given in the following table:

Table 5.1 Variances for plots as in Figure 5.3

Plot	Description	Variance
a	Opposite paired 4-electrode	3.4
b	2-electrode	0.84
c	Adjacent paired 4-electrode	1.24
d	Adjacent paired 4-electrode	1.61

Looking at Figure 5.2b this configuration shows a promising large area of homogeneity and relatively large changes to the capacitance in this area. This is backed up by the lower variance compared with the other configurations. Figure 5.2c and d also have areas of homogenous change in capacitance but are disrupted by large peaks. This is also reflected in their higher variances.

5.3 Effect of void distribution

The results of the different void distributions for a 2-electrode sensor are shown in Figure 5.3. To calculate the void fractions equation (3.3) was used.
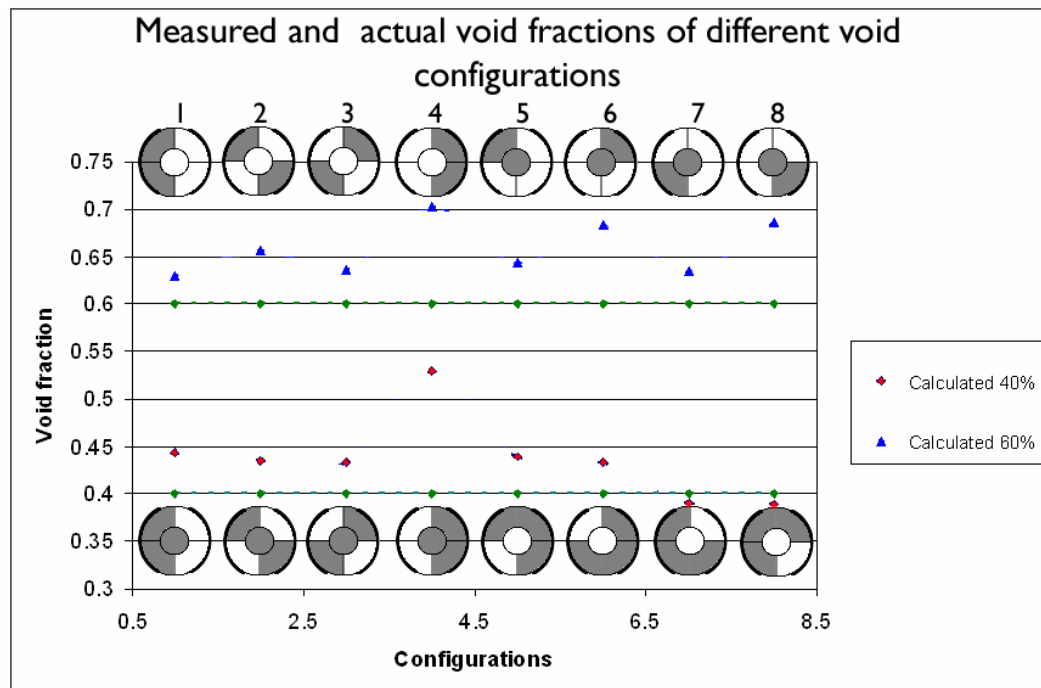
Figure 5.3 Void fractions for different void distributions at 60 and 40% using the 5 segment void model with a 2-electrode sensor. The gray blocks show where the segments have been placed.

In general the calculated void fractions were much higher than was expected. A reason for this could be the fact that equation (3.3) is only a approximation for series void distributions in a homogenous electric field. This could result in a constant offset in the calculated results. It also appears that void distributions with the most void on the left hand side of the sensor have the biggest deviation from

the expected values. Theoretically configurations 1 and 4 are symmetrically identical and should produce the same results. This is also the case for 6 and 7. This would suggest that one electrode (on the right) has a larger effect on the perspex than the other electrode. This is confirmed in Figure 5.2b where the relative change in the capacitance is on average slightly higher on one side than on the other. Configuration 4 gives the worst results for both 60 and 40 percent void with relative errors of respectively 15% and 35%. For the other configurations the measured values stay within a relative error of 13%.

5.4 Bubbly void distribution

Figure 5.4 shows the results for the different bubble distributions, again for the 2 electrode sensor. As in the previous experiment there appears to be a constant offset. The measured values tend to be higher than the expected values.
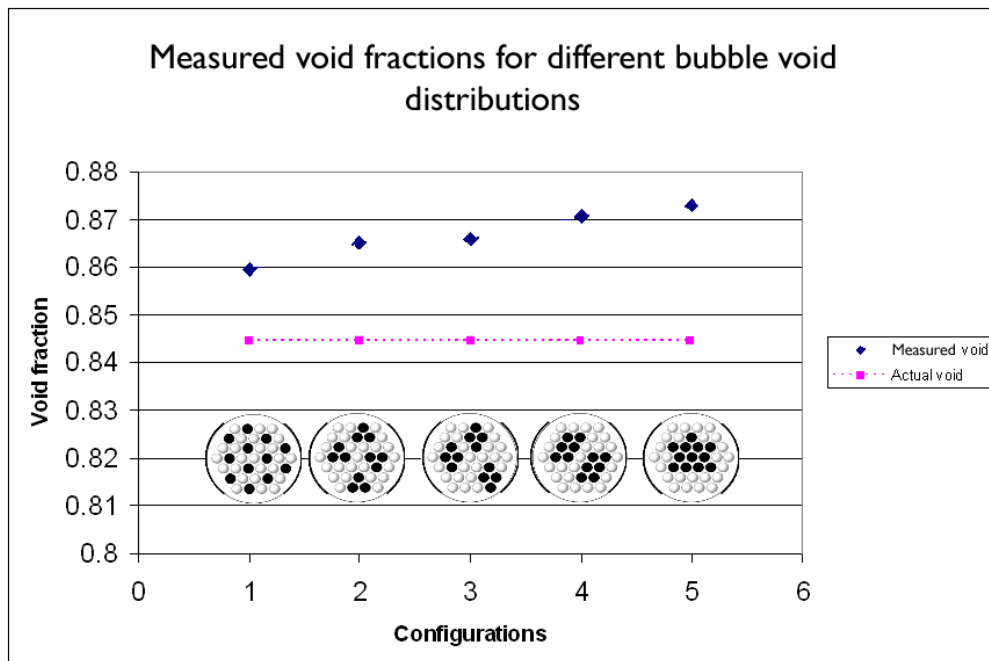
Figure 5.4 Void fractions for different bubble size using the rod void model with a 2-electrode sensor. The black dots indicate where the rods have been removed

There appears to be a correlation between the size of the bubbles and the measured void fraction. This could be due to the fact that for the smaller bubble distributions there are more rod elements closer to the edges of the pipe. As we had seen in Figure 5.2 the effect of the rods nearer to the outside of the pipe have a larger effect on the capacitance. Configuration 1, 2 and 3 have respectively 6, 3 and 3 removed rod elements on the outside where as 4 and 5 have none. The larger change in capacitance means a larger f_m. From equation (3.3) we see this would result in a smaller value for the void fraction. The relative errors for these measurements are much better than for the previous experiment with all measured values being within a relative error of 3%. The most homogenously distributed bubble configuration (1) had an error of just 2%.

5.5 Measurement error

The capacitance sensor is very sensitive to any change in the position of the wires connecting the electronics because these constitute a major part of the parasitic capacitance. To determine the measurement error, ten repeated measurements will be done using the 5 segment void model on three void configurations. The three configurations considered were:

- no Perspex ($\alpha=1$) for f_v,
- completely filled with Perspex, all 5 segments in ($\alpha=0$) for f_l
- the central rod of 21.8 mm of Perspex missing ($\alpha=0.214$) for f_m

Equation (3.3) was once again used to calculate the void fraction. The results of the repeated measurements are shown below:

Table 5.2 Results of repeated measurements

Calculation	Standard deviation, σ
$\dfrac{f_l}{f_v} = 0.9649$	0.0002
$\dfrac{f_l}{f_m} = 0.99241$	0.0001
$\alpha = 21.6\%$	0.21%

Because $\dfrac{f_l}{f_v}$ was determined to be 0.9649, this indicates that the full sensor range between zero and 100% void is just some 3.5% of the total capacitances, which means the rest of the capacitance comes from parasitic capacitances from, for example, the guard and the wires. The void fraction at 21.4% was calculated to be 21.6% with a standard deviation over the 10 measurements of 0.21%. This gives a detection limit of 0.4%. For this type of void distribution (central void) equation (3.3) seems to hold very nicely.

During the measurements it became apparent that the sensor needed a certain amount of time to produce stable results. After initially turning the sensor on it would take 20 minutes to reach a state of steadily climbing values. After this the measurements would continue to climb at a rate of about 0.06 pF per hour. This corresponds to a change in void fraction of 4% in 1 hour. Figure 5.5 shows the capacitance as a function of time for the first few hours after the having been turned on.

Capacitance measurement over time after turnig on the sensor
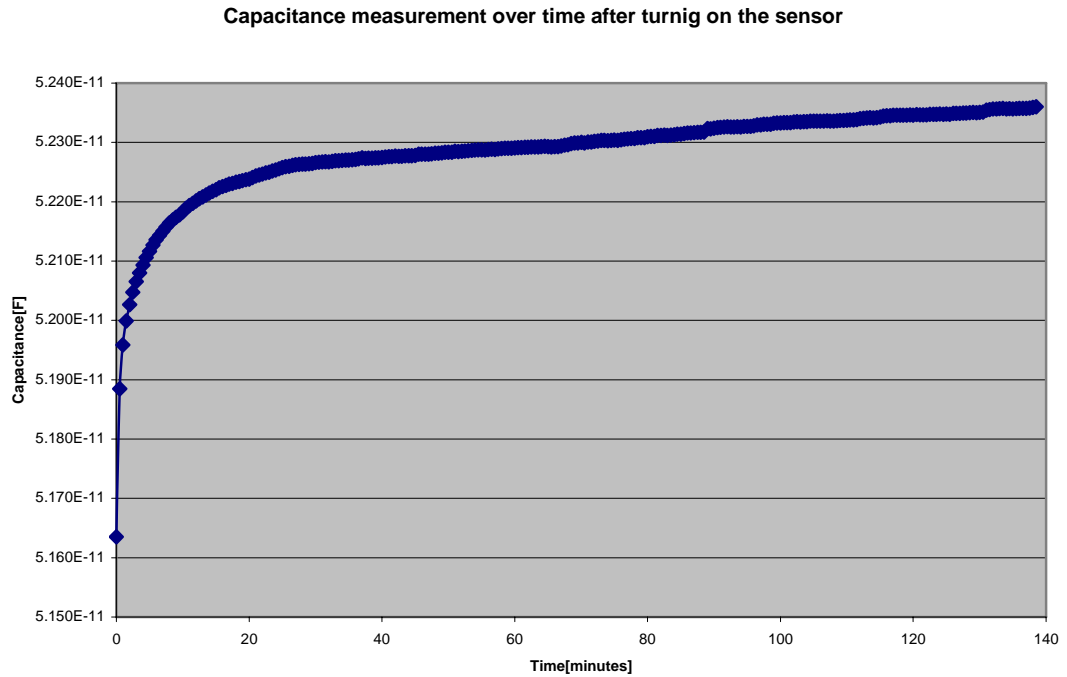
Figure 5.5 Instability of sensor after turning it on with filled 37 rod configuration and a stable room temperature.

After many hours the sensor would reach a stable value. To overcome this problem the sensor was left on at all times. To account for this instability the temperature dependence of the circuitry in the sensor electronic must be investigated. It is possible that the electronics behave differently as they heat up due to the currents that flow though them. It is also possible that a small change in the external temperature could have an effect on the sensor although the room temperature remained a stable 18 degrees C during this experiment. This strange instability could be investigated further in any future research into this measurement technique.

6 Conclusions

6.1 Conclusion

One of the void fraction techniques for the GENESIS project is one based on capacitive measurements. Capacitive techniques provide a quick, simple non-intrusive solution for determining void fractions. There are two important factors that influence the dependence of the capacitance of the sensor on the void fraction. The first is the distribution of the two phases within the pipe and the second is the homogeneity of the electric field between the electrode plates.

The electric field distribution within and around the sensor could be investigated by simple computer models. These showed that a 2-electrode sensor provided the best homogenous electric field distribution.

A Perspex model made it possible to determine important properties for optimisation of the sensor. It has been shown that the distribution of the void has a large impact on the dependence of the void fraction on the capacitance. If the void distribution is known, however, it is easy to calibrate the sensor to give more accurate results. The second important factor can be minimised by careful sensor design. From these experiments it was also evident that for an even distribution of the electric field the 2-electrode sensor gave the best results.

The relative accuracy of the sensor is estimated to be 10-15% if a proper calibration is performed and the void distribution is unknown. However for extreme cases of void distribution at lower void fractions this climbs up to 35%. The detection limit of the sensor is 0.4%.

In a bubbly flow distribution the size of the bubbles also influences the out come of the measurements. Improving the homogeneity of the sensor would remove this dependence on bubble size and distribution to produce more predictable results. The relative error $(2 - 3\%)$ for the bubbly flow distributions was much lower than for the other distributions. This might suggest that the sensor is better suited to homogenous void distributions at higher void fractions.

6.2 Suggestions for further research

The perspex model was ideal for initial testing of the basic properties of the capacitive sensor however it is a static model. The implementation of the sensor is intended to be used in a highly dynamic situation. Further characteristics of the sensor can be investigated by using a more realistic model. A pipe with rising bubbles that vary in size and speed is easily implemented. By filling a pipe with a liquid and injecting bubbles at a location under the sensor bubbly flow could be investigated. Different bubble sizes could be achieved by stirring the liquid up with a mixing device. By creating a loop and pumping the water around at different speeds whilst still injecting the bubbles one could vary the speed of the

bubbles and create an even better simulation of the sensors eventual situation. This would provide enough scope for further research.

The temperature dependence of the sensor has not been investigated at all. The dielectric constant of a medium is often dependent on the temperature which would have significant consequences for the capacitive sensor. By carefully controlling the sensor's surrounding temperature one could investigate this in more detail.

An investigation into the performance of differently shaped electrodes could also provide interesting further research. Other publications (see Abouelwafa, Kendall [3] and Elkow, Reskallah [5]) show that helically shaped electrodes provide results that correspond well with expected values for certain flow patterns.

7 References

[1] Kok H.V., *"Capacitive measurement technique for void fraction measurements in a rod bundle geometry"* Interfaculty Reactor Institute, Delft University of Technology.

[2] Griffiths D.J., *"Introduction to Electrodynamics"* Third edition, Prentice Hall.

[3] Abouelwafa M.S.A., Kendall E.J.M., *"The use of capacitance sensors for phase percentage dtermination in multiphase pipelines"* IEEE Transactions on Instrumentation and measurement, VOL. im-29, no.1 March 1980.

[4] Baxter, Larry K. *"Capacitive sensors; design and applications"* IEEE, New York 1997

[5] Elkow K.J., Reskallah K.S., *"Void fraction measurements in gas-liquid flows using capacitive sensors"* Meas. Sci. Technol. 7 (1996).

8 List of symbols

V	Electric potential
$\vec{E}$	Electric field
Q	Charge
σ	Surface charge density
ρ	Volumetric charge density
$d\vec{l}$	Infinitesimal distance unit
$d\tau$	Infinitesimal volumetric unit
r	Distance from origin to point r
ξ	Distance from point r to integration unit
C	Capacitance
ε_r	Dielectric constant of a medium
ε_0	Permittivity of free space(vacuum)
ε_{eff}	Effective dielectric constant
$\vec{P}$	Polarisation
σ_b	Bound surface charge
σ_f	Free surface charge
$\hat{n}$	Unit vector normal to the surface
α	Void fraction
C_l	Capacitance of the sensor filled with only liquid
C_m	Capacitance of the mixture of the two phases
C_v	Capacitance of the sensor filled with only vapour
f_l	Frequency of the sensor filled with only liquid
f_m	Frequency of the mixture of the two phases
f_v	Frequency of the sensor filled with only vapour